Far-Ultraviolet Observations of the Galactic Supersoft Binary RX J0019.8+2156 (QR Andromedae)

Hutchings, J.B.; Crampton, D.; Cowley, A.P.; Schmidtke, P.C.; Fullerton, A.W.

National Research Council Canada   Conseil national de recherches Canada

Canada

FAR-ULTRAVIOLET OBSERVATIONS OF THE GALACTIC SUPERSOFT BINARY RX J0019.8+2156 (QR ANDROMEDAE)[1]

J. B. HUTCHINGS,[2] D. CRAMPTON,[2] A. P. COWLEY,[3] P. C. SCHMIDTKE,[3] AND A. W. FULLERTON[4,5]

ABSTRACT

Far-Ultraviolet Spectroscopic Explorer spectra were obtained of the supersoft X-ray binary RX J0019.8+2156 (QR And) during 16 consecutive spacecraft orbits, covering the binary orbit ($P = 15.85$ hr) with about 0.2 phase overlap. The spectrum is dominated by strong H_2 absorption (column density $\sim 10^{20}$ g cm^{-2}), which appears at the velocity different from other interstellar absorption lines and may be partially circumbinary. This absorption makes study of spectral features from the binary system difficult. The only well-detected emission lines are He II $\lambda 1085$ and O VI $\lambda 1032$ (the other line of the O VI doublet, at 1037 Å, is largely obscured by strong H_2 absorption). The O VI shows a P Cygni profile that varies in velocity and strength with binary phase. We compare this with similar changes seen in Balmer line profiles. We extract the far-ultraviolet (FUV) light curve and compare it with the optical light curve. There is an eclipse in both wavelength regions, but the FUV minimum lasts much longer, well beyond the visible light egress. The FUV results are discussed in connection with the binary model and mass flows within the system.

Key words: binaries: close — ISM: jets and outflows — stars: individual (RX J0019.8+2156 = QR And) — ultraviolet emission — X-rays

1. INTRODUCTION

RX J0019.8+2156 (hereafter called by its variable star designation, QR And) is one of the few identified Galactic supersoft X-ray binaries, although numerous examples have been found in the Magellanic Clouds and M31 (see Greiner 1996). The system was first noted in the *ROSAT* All-Sky Survey and described by Beuermann et al. (1995). They found this 12th magnitude system shows ~ 0.5 mag eclipses and radial velocity variations that fit an orbital period of 15.85 hr. Archival photographic plates show the orbital period has been stable for over 40 years (Greiner & Wenzel 1995), although there are irregular changes of a few tenths of a magnitude in the overall brightness level of the system (e.g., Cowley et al. 1998; Deufel et al. 1999).

The system is at Galactic latitude $-40°$ and hence shows little evidence of interstellar reddening, with mean $U - B \sim -0.7$ (Beuermann et al. 1995) and quite weak interstellar lines of Ca II and Na I (McGrath et al. 2001). This, with the mean absolute magnitude of supersoft binary systems, places its distance at ~ 2 kpc, so it lies well out of the Galactic plane.

Optical spectra show very strong emission lines of He II (virtually all the He II lines in the Multiplet Table are identified). Balmer absorption lines are present through about half the orbital cycle and indicate a strong outflow of material with velocities of about -200 to -600 km s^{-1}.

Like several other supersoft X-ray binaries, QR And also shows bipolar emission-line jets (velocity about ± 800 km s^{-1}) in He II ($\lambda 4686$) and the lower Balmer lines (e.g., Becker et al. 1998; Cowley et al. 1998; Deufel et al. 1999). These jet features come and go on timescales of weeks to months. Since the Balmer outflow is phase dependent (and persistent?), this is likely a constant disk flow that is not strongly related to the jet activity.

There has been some disagreement about the appropriate model for QR And, with various authors deriving quite different values for the orbital inclination and hence the stellar masses. Beuermann et al. (1995) concluded that the inclination must be quite low ($i \sim 20°$), based partially on the assumptions that the masses are similar and consistent with a white dwarf. On the other hand, Meyer-Hofmeister et al. (1998) analyzed the light curve and presented models that indicate an inclination near $i = 55°$, while Tomov et al. (1998) suggested an even larger value ($i \sim 79°$), also based on the light curve. The adopted inclination is important since it ultimately confines the range of possible masses and hence the model and evolution of the system. From an analysis of the emission-line velocities and those of the bipolar jets, Becker et al. (1998) found that the jet lines show the same velocity amplitude and phasing as He II 4686 Å and hence concluded that the He II lines must reveal the motion of the compact star where the jets originate. Further, from analysis of the outflow line profiles they found that the orbital inclination must lie in the range $35° < i < 60°$. For the purpose of our discussion below, we have adopted these conclusions of Becker et al. and assume a model similar to that discussed by Meyer-Hofmeister et al.

O VI emission ($\lambda\lambda 3811$, 3835, and 5290) is found in all supersoft X-ray binaries and is potentially interesting as its high ionization may indicate an origin close to the accretion disk center. However, study of these lines is compromised by blends with He II at 3813 and 3834 Å and with [Fe XIV] at 5303 Å. This suggested that it would be particularly interesting to observe the supersoft systems in the far-ultraviolet with the *Far-Ultraviolet Spectroscopic Explorer* (*FUSE*)

TABLE 1

FUSE Observations of RX J0019.8+2156

Orbit	Photometric Phase[a]	HJD (mid) 2,451,700+	Exposure (s)
1	0.475	52.922	2481
2	0.584	52.993	2191
3	0.694	53.066	1871
4	0.799	53.135	1590
5	0.907	53.206	1310
6	0.966	53.246	418
7	0.013	53.277	1160
8	0.075	53.318	850
9	0.120	53.347	920
10	0.184	53.389	1220
11	0.227	53.418	701
12	0.293	53.461	1721
13	0.327	53.478	1320
14	0.414	53.541	3461
15	0.519	53.610	3461
16	0.622	53.679	3301

[a] Ephemeris: T_0 = HJD2,449,987.8459(16) + 0.6604645(14) E days (McGrath et al. 2001).

since the O VI resonance lines (1032 and 1037 Å) lie within its wavelength range.

2. *FUSE* OBSERVATIONS

An overall description of the *FUSE* data is given by Sahnow et al. (2000). Our *FUSE* observations were carried out during 16 successive spacecraft orbits on 2000 July 27–28. The large apertures (30″ × ″30) were used. No unusual anomalies were apparent during the observation sequence. The observations were taken in time tag mode, and the 16 separate spectra cover slightly more than one binary orbit. Table 1 lists the details of the observations.

The spectra were processed by the CALFUSE pipeline and retrieved from the archive. Later, the data were reprocessed using an updated version (1.8.7) of the pipeline processes. The results were the same to within about 1%.

Surprisingly, the spectra were found to be heavily absorbed by molecular hydrogen (H$_2$). The amount of absorption is characteristic of more reddened targets [$E(B-V) = 0.5$ or more], whereas, as noted above, QR And has quite blue colors. The spectra also contain airglow emissions (see Feldman et al. 2001) that are much stronger on the daylight side of the *FUSE* orbit. Spectra 6, 8, 10, and 12 were taken almost entirely during orbital night, and thus they provide a way to assess the airglow contamination of the other spectra. Fortunately, the spectral region near the O VI λ1032 emission line is free of airglow lines, so that our analysis of this region could be performed on data from both orbital night and day without editing.

3. SPECTRAL ENERGY DISTRIBUTION AND H$_2$ ABSORPTION

To assess the contamination due to H$_2$ absorption, we used simple absorption models with a range of column densities. We also derived an empirical absorption model by using a median spectrum of the region of interest around the O VI resonance lines. The 1032 Å line is free of strong H$_2$ absorptions, but the 1037 Å line is almost completely overlaid by saturated absorption.

Figure 1 shows the average spectrum with different amounts of smoothing and airglow removal, as well as the
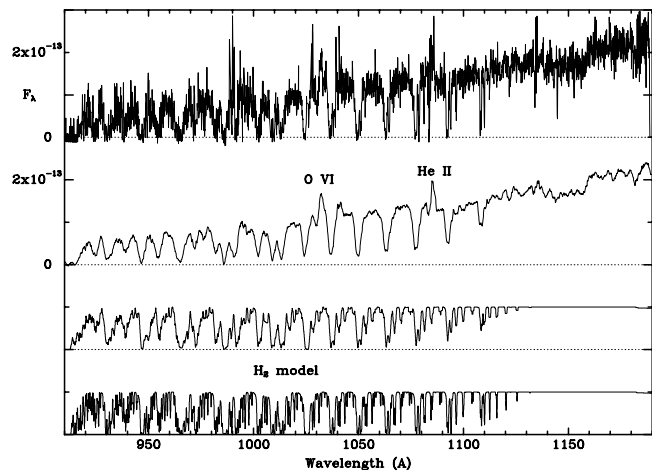

FIG. 1.—*Top two plots*: Average *FUSE* spectrum of QR And with different amounts of smoothing and airglow removal; *bottom two plots*, for comparison, the H$_2$ model absorption with two different smoothings.

H$_2$ model from our grid that fits it most closely. The H$_2$ absorption strength in the *FUSE* wavelength range is loosely correlated with $E(B-V)$ and was compared with several B0 stars with $E(B-V)$ ranging from 0.15 to 0.5 mag, which had been observed with *FUSE*. The values for QR And correspond to values of $E(B-V) \sim 0.5$. However, Beuermann et al. (1995) estimated a value of $E(B-V) \sim 0.10$ for QR And, based on the strength of its 2200 Å absorption feature. The colors of QR And ($U-B = -0.7$ and $B-V = 0.01$) also show the system to be very blue, so the $E(B-V)$ cannot be 0.5 and the H$_2$ absorption strength is unusually high for the reddening. Since the system is losing matter via disk and jet outflow, it is worth considering whether some of the H$_2$ absorption is due to material surrounding the binary. We estimate the column density causing the H$_2$ absorption to be $\sim 10^{20}$ cm^{-2}. Beuermann et al. (1995) estimated an absorbing column of 4×10^{20} H atoms cm^{-2} from *ROSAT* data for a combination of Galactic foreground absorption plus any possible intrinsic absorption.

To determine whether the H$_2$ absorptions are interstellar or circumstellar, we compared their velocities with Ca II and Na I interstellar lines and with QR And's systemic velocity, both derived from optical spectra. From the *FUSE* spectra we measure the heliocentric velocity of H$_2$ features near the O VI lines to be -16 ± 2.5 km s^{-1}, with no variation from spectrum to spectrum. The absolute wavelength precision depends on placing the star accurately in the (guided) LiF1 channel aperture. A precision of 1″ is expected, which corresponds to ± 3.4 km s^{-1}. To check the *FUSE* wavelength zero point further (possibly due to grating movement uncertainty), we measured the Lyβ airglow wavelength. This tracks the orbital velocity of *FUSE* along the bore sight to within 2 km s^{-1}, so we conclude that velocities are correct as measured.

A Multiple Mirror Telescope spectrum obtained 1995 October 12 shows the mean velocity from interstellar absorption lines of Ca II and Na I to be $+4 \pm 4$ km s^{-1}. McGrath et al. (2001) found the systemic velocity of QR And to be about -41 ± 3 km s^{-1} (Beuermann et al. 1995 gave -59 ± 2 km s^{-1} from lower resolution data). The measured H$_2$ velocity of -16 km s^{-1} lies between the interstellar medium (ISM) and binary velocities. In view of the

unusual H_2 strength, it thus seems likely that it is partly associated with the binary system—perhaps formed during a planetary nebula (PN) episode and well-removed spatially from the current ionizing radiation from supersoft X-ray activity.

4. FAR-ULTRAVIOLET AND OPTICAL LIGHT CURVES

The *FUSE* data were used to construct the FUV light curves shown in Figure 2. *FUSE* consists of four separate telescopes that are kept co-aligned by compensating for modeled mechanical distortions around the orbit (e.g., Moos et al. 2000). Only one telescope (LiF-1) is used for tracking. The extraction of signal is thus uncertain in the other three telescopes if the signal is weak and the position of the target in the (30″) aperture drifts by a great deal. The LiF1A (longer wavelengths) are also subject to a detector wire shadow (the "worm") that may affect photometric accuracy. However, the LiF2A (longer wavelength: 1090–1180 Å) channel has little drift and the highest signal level. Thus, we used the fluxes from the LiF1A (990–1080 Å) channel and the LiF2A channel to derive two independent light curves. The continuum fluxes were estimated by summing these spectral regions after removing airglow lines and interpolating across the deep H_2 absorptions. These are shown as a function of phase in Figure 2, displayed as magnitudes. There is good correspondence between the two ultraviolet regions. The count rates for all channels are steady and show no variations that might indicate the star was drifting out of the aperture. The spectral images show that the extraction windows appear to cover the data well. In the binary phases in which *FUSE* observations overlap (phases 0.5–0.7), the fluxes are in good agreement.

The *FUSE* fluxes were rechecked by one of us (A. W. F.) on the raw data using the current version of CALFUSE (1.8.7). The calibrated spectra include the total counts associated with each pixel (i.e., the sum across the width of the spectrum in the spatial direction). A light curve from the total signal over the interval 1102–1133 Å was derived from the LiF1B channel. This region does not have any strong airglow lines and avoids the LiF1B channel "worm." The result is essentially the same as the 1090–1180 Å LiF2A curve shown in Figure 2. To check CALFUSE further, spectra for 5 minute intervals were extracted from the raw data, and count rates were determined over the same 1102–1133 Å wavelength region. These light curves are also very similar to the FUV light curves shown in Figure 2.

Comparing the two FUV light curves in Figure 2, we find that overall amplitude is larger by ~0.03 mag in the longer wavelength channel. This is likely to be caused by H_2 line blanketing that lowered the continuum in the shorter wavelength region where the absorptions are more crowded (see Fig. 1), rather than being a real color change. We note that the visible light shows almost no color changes through eclipse (e.g., Cowley et al. 1998; Deufel et al. 1999).

For comparison of the optical and far-ultraviolet fluxes, Figure 2 shows two V-band light curves, together with the two derived from the *FUSE* data. The nearly complete optical light curve (*filled circles*) was obtained in 1995 September and is fully described by McGrath et al. (2001). It is plotted with 9 point smoothing applied. In the unbinned optical data, flickering is present throughout the orbital cycle, and quasi-periodic variations ($P \sim 1.8$ hr) are prominent at orbital phases 0.2 to 0.6. The second optical light curve (*open circles*) shows V data taken on 2000 July 28 by one of us (P. C. S.) at Braeside Observatory in Flagstaff, Arizona, with monitoring beginning just hours after completion of the *FUSE* observations. The orbital phase coverage is rather limited, but it includes most of primary eclipse. The short-term fluctuations are of much smaller amplitude than in the 1995 data. In 2000, QR And was ~0.1 mag brighter than in the 1995 data, but variations in the mean brightness level are well known in this system (cf. Will & Barwig 1996; Matsumoto 1996; Cowley et al. 1998; Deufel et al. 1999). The optical data shown here illustrate the typical behavior of this source.

There are very obvious differences between the optical and FUV light curves in the phases following minimum light. While the ingress is similar in both wavelength regions, the FUV light curve shows a minimum that lasts from phase 0.95 through 0.25, much longer than the minimum observed in optical light. Thus, we appear to have an eclipse of the hottest regions of the disk that extends well beyond that of the cooler regions seen in optical wavelengths. If this extended minimum is real, it could indicate important disk structures in the system that presumably affect the FUV radiation. However, we would really like to observe another minimum to be certain there was no *FUSE* instrumental problem. The "secondary eclipse" dip present in the visible light curve is not seen in the FUV, but a small dip does occur at phase ~0.6.

If the FUV extended eclipse represents a permanent feature, we might expect to find a gradual change in the light curve as one observes at progressively shorter wavelengths. The best we can do at the present time is to examine other light curves available in the literature. Beuermann et al. (1995) show light curves at 1400–1500 Å and X-ray data from the *ROSAT* Position Sensitive Proportional Counter. Replotting these data with a more extended vertical scale we find both the duration of minimum and the phases of ingress and egress to be consistent with our optical light curve and that of Will & Barwig (1996). Similarly the *IUE* data shown by Gaensicke, Beuermann, & de Martino (1996) for 3000 and 1250 Å when replotted also show similar
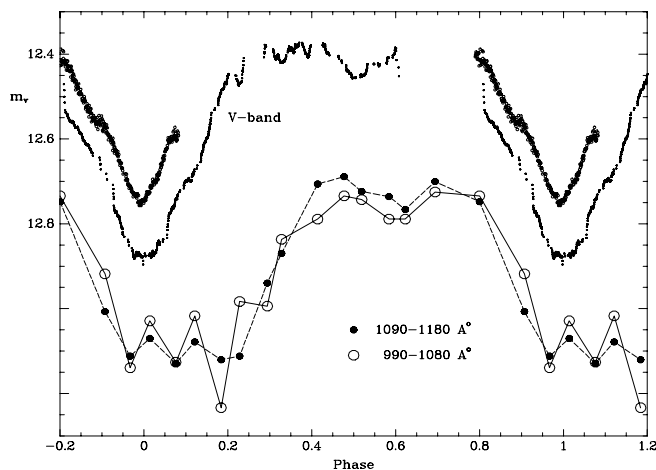

FIG. 2.—Light curves for QR And. The open circles (*upper curve*) represent V data obtained on UT 2000 July 28, only a few hours after the *FUSE* observations ended. The filled circles represent the V data of McGrath et al. (2001). It is known that this binary shows variations of a few tenths of a magnitude in its mean brightness level (e.g., Cowley et al. 1998; Deufel et al. 1999). The lower two curves represent the *FUSE* light curves extracted from different wavelength regions, as indicated. Phases are computed using the ephemeris given by McGrath et al.

phases of ingress and egress and duration of minimum flux. We were unable to find any indication from published ultraviolet data of other extended-duration eclipses such that as seen in the *FUSE* data. However, Gaensicke et al. (2000) show *ROSAT* HRI X-ray data obtained between 1997 December 2 and 1998 January 10 in which there is no evidence of any orbital variation. Thus, changes do occur in QR And that severely modify the light curve. Furthermore, Meyer-Hofmeister et al. (1998) found that important changes in the disk rim structures can occur on timescales as short as the orbital period. However, without additional *FUSE* data, we don't know whether the extended minimum we observed in the FUV light curve was a transient event or due to a more permanent structure in the binary system.

5. FUV SPECTRUM

The spectra were examined carefully for the presence of high-ionization lines in the *FUSE* range. While the H_2 contamination makes this difficult, we find no evidence of N III, C III, S IV, Si V, or P V. However, O VI is clearly present and has a complex and variable line profile that we discuss in detail below. The only other line we detect is He II at 1085 Å. This line is close to two airglow lines of N II, but both the median of all spectra and the sum of the night spectra show there is a broad He II emission line present, in addition to the narrow and variable airglow lines. Because of the airglow contamination and the weakness of He II, we are unable to study its behavior as a function of binary orbital phase. Nevertheless, it is clear that the line does not have the P Cygni absorption profile found in the O VI lines. This is consistent with the purely emission profiles of the visible Pickering He II lines reported by McGrath et al. (2001). We note that in ORFEUS II observations (900–1200 Å) no stellar emission lines were detected (Gaensicke et al. 2000).

In the optical region, lines of C III and C IV (and possibly N III and N V) are weakly present (McGrath et al. 2001), but *IUE* spectra of QR And show no evidence of the resonance lines of C IV at 1550 Å (Beuermann et al. 1995). The only emission feature in the *IUE* data is He II $\lambda 1640$. In the *FUSE* spectra, C III at 1175 Å is not detected, even though it is clear of H_2 and airglow. We set an upper limit on its equivalent width of less than 0.1 Å. It appears that carbon, and possibly nitrogen, have low abundances in QR And.

5.1. O VI

The strongest emission line in the *FUSE* range is O VI $\lambda 1032$. This whole feature is fortunately free of airglow or major H_2 absorption (there are some weak narrow absorptions, but they are comparable to the noise levels in individual spectra and very much narrower and weaker than the stellar lines). The line has a P Cygni profile that changes around the binary orbit, as shown in Figure 3. By subtracting an H_2 model and looking at differences from the median of all spectra, we can also see the edges of the absorption and emission of the O VI 1037 Å line, which gives us added confidence that the changes we see in the 1032 Å line are real.

The extensive spectral coverage of the optical region by McGrath et al. (2001) shows that the lines near Balmer wavelengths have P Cygni profiles that change markedly around the orbit. (Note that the emission portion of these lines is a blend of H + He II, as one can tell by comparing their strengths with the nonblended, adjacent He II Pickering emission lines. However, the variable-strength absorption component is due only to H.) Figure 3 shows the changes in both the *FUSE* O VI line and the optical "Balmer" lines during similar phases (computed using the optical ephemeris of McGrath et al.) The *FUSE* data are
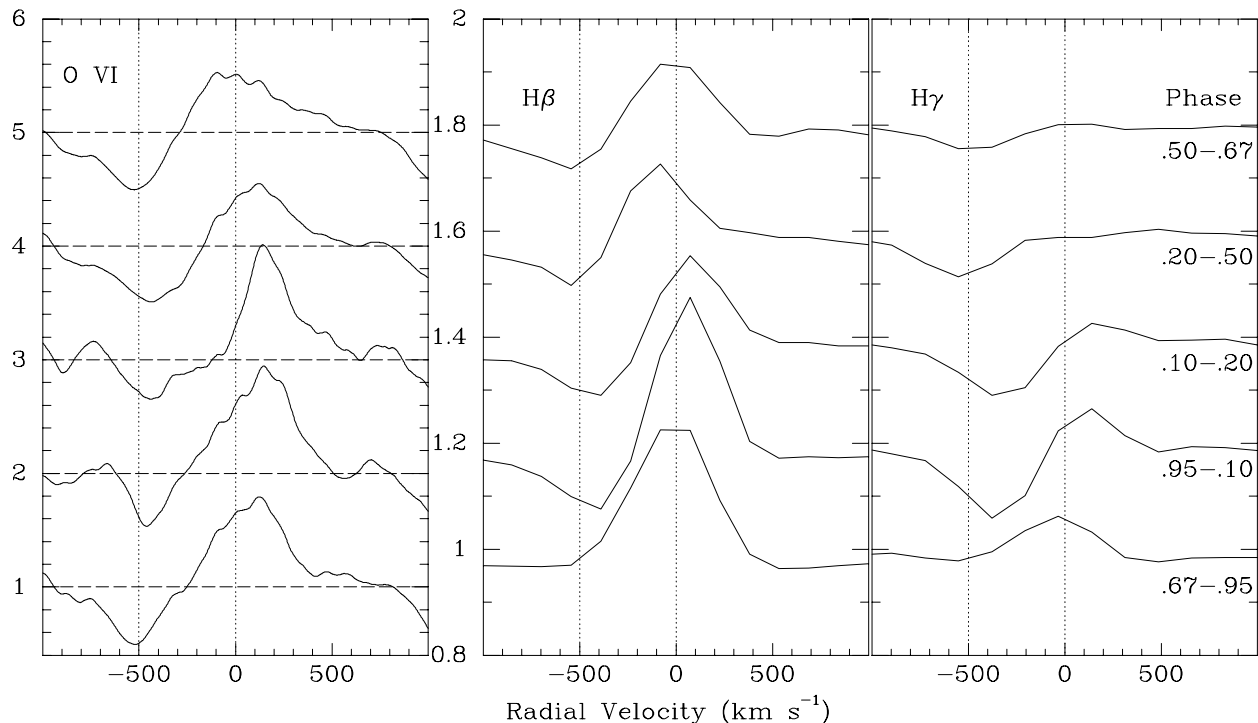

Fig. 3.—Line profiles of O VI $\lambda 1032$ binned through the orbital phases indicated. These are compared with line profiles of Hβ and Hγ in the same phase bins (from the data of McGrath et al.). The *FUSE* data (*left*) have been heavily smoothed to spectral resolution ∼1 Å; the optical data (*right*) had an original resolution of ∼5 Å, but many spectra have been averaged together. The vertical scales are in units of the local continuum.
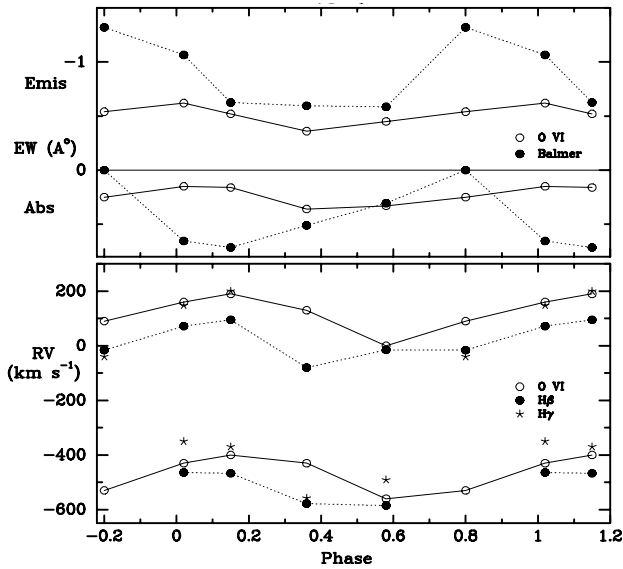
FIG. 4.—Velocity and equivalent-width measurements from *FUSE* and optical spectra binned as in Fig. 3. The measurements are made with respect to the continuum levels plotted in Fig. 3. *Top*: Mean of Hγ and Hβ plotted to simplify the diagram. The Balmer velocities are not corrected for the He II blending, which would be -60 km s^{-1} for equal contributions of H and He II to the emission.

smoothed by 91 points, which makes the resolution comparable to the optical, without losing the significant changes in the broad line profiles. To compare the O VI and "Balmer" lines, the optical spectra were averaged from numerous spectra within the phase bins specified, but were not smoothed. The profiles in Figure 3 were normalized to the local continuum, and measurements were made of the centroids and fluxes of the emission and absorption components as shown in Figure 4. The values plotted in Figure 4 have measured total scatter of $\pm 20\%$ for the EW values, and velocities are reproducible to ~ 50 km s^{-1}, taking into account uncertainties in continuum fitting.

The absorption outflow velocities are similar for all three lines shown in Figure 4, but the variations in absorption strength differ. O VI has absorption at all phases, while little or no Balmer absorption is present from phases 0.7 to 0.0. The O VI and H absorption strengths thus show no binary phase correlation in Figure 4, while the O VI emission and absorption do follow the phase variations of the Balmer lines, albeit with a smaller amplitude. This suggests that there may be significant azimuthal variations of the ionization of the outflowing material. In this connection we note that *FUSE* data show anomalous O VI presence in the outer regions of OB star stellar winds (Crowther & Bianchi 2001) whose ionization may be connected with X-ray flux. Further work is needed to understand these phenomena properly.

If the velocity of the O VI emission is due to orbital motion of the compact star, maximum velocity should occur at photometric phase 0.25. However, the maximum occurs $\sim 0.1P$ earlier, almost certainly due to the very strong P Cyg absorption present between phases 0.0 and 0.2. The O VI velocities are very similar to those found by McGrath et al. for the blended H + He II emission lines. These authors suggest that only the pure He II lines (i.e., those with no trace of overlying H absorption) reveal the orbital motion of the compact star, the same conclusion reached by Becker et al. (1998). The variable strength of the hydrogen absorption modifies the emission-line profiles, hence distorting their velocity curves.

Changes in the line profiles are shown in Figure 5. Differences from the phase bin showing emission-only "Balmer" lines are plotted, so the figure shows the changes in the
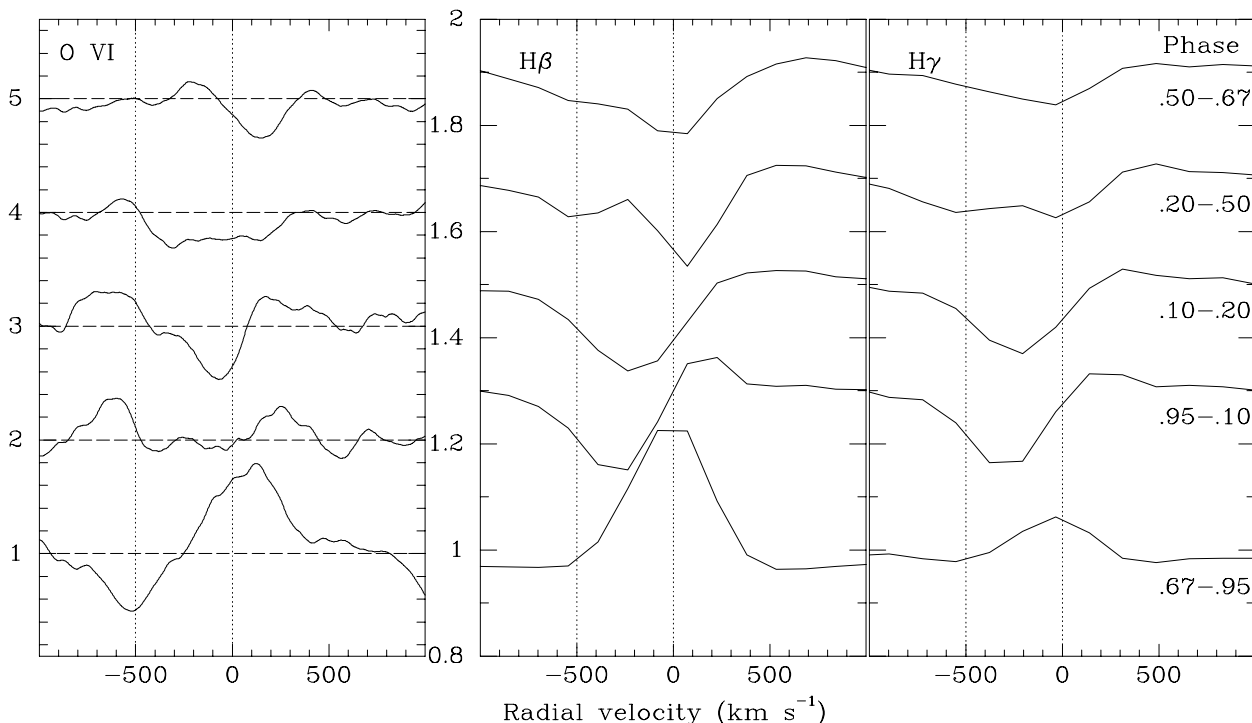

FIG. 5.—Similar to Fig. 3, but showing changes in profiles from the 0.67–0.95 phase bin, where Balmer absorption is not seen. The phase 0.67–0.95 profiles are shown in the lowest plots. This figure illustrates the changes in the absorption components with binary phase.

absorption with phase. The O VI absorption is more complex and is seen at all binary phases. It is weakest during the low parts of the FUV light curve, suggesting that the O VI absorption is associated with the FUV continuum source.

6. DISCUSSION AND SUMMARY

The optical spectra of McGrath et al. show that there are significant outflows from the system, with strong azimuthal variations. Generally speaking, the outflows have velocities of several hundred kilometers per second and are seen most strongly through mideclipse and egress, but they are not seen during eclipse ingress. In the *FUSE* data, the O VI resonance lines show an outflow of very hot gas at all phases, but with velocities similar, although somewhat lower, to the Balmer absorption.

The emission and absorption features in O VI and H + He II show similar velocity changes with binary phase. These are not the same as the pure He II emission velocity curves, which appear to trace the binary orbital motion (e.g., Becker et al. 1998; McGrath et al. 2001). Thus, the wind from the binary has azimuthal velocity variations. The relative absorption strength also changes with binary phase, which may indicate azimuthal ionization changes. The production of O VI in OB stars is anomalous and may have some connection with X-ray ionization, which could also be occurring in QR And.

We find that the high H_2 absorption column, which is anomalous for the unreddened system color, has a different velocity from the atomic interstellar lines, lying between the ISM and assumed binary systemic velocity. We suggest that it may partially arise in a circumbinary location, possibly formed during the presumed PN episode that occurred prior to the present evolutionary stage. We note that circumbinary H_2 is detected around some planetary nebulae and that other degenerate binaries we are studying with *FUSE* do not show appreciable H_2 absorption.

Finally, the very odd FUV light curve shows an extended eclipse minimum lasting about one third of the orbit, although only one eclipse was observed by *FUSE*. While it may be tempting to connect the extended FUV eclipse with variable H_2 absorption, the FUV light curve was derived from the longer *FUSE* wavelengths, which are free of H_2 absorption. Furthermore, we have determined that there is no change in the column density of H_2 or its velocity during these phases. The difference between the visible and FUV eclipse might be explained by a UV-bright spot on the rim of the disk, where a mass transfer stream impacts it (e.g., models by Meyer-Hofmeister et al. 1998). The off-axis location of such a spot could give rise to an extended eclipse in the FUV. Such a model would imply that the effect becomes more visible as the wavelength of observation decreases from visible to FUV. Our examination of archival photometry at UV and X-ray wavelengths suggests that the light curve may show large long-term changes.

If the O VI line profile (both emission and absorption) arises in part (or entirely) at this UV-bright location, the observed phasing of the O VI radial velocities is qualitatively as expected. One can also imagine different outflow velocities for O VI, as observed, if the line arises primarily from this location rather than from the entire disk. The lack of hydrogen absorption from phases 0.65 to 0.95 might occur if the region around this hot spot is highly ionized.

REFERENCES

Becker, C. M., Remillard, R. A., Rappaport, S. A., & McClintock, J. E. 1998, ApJ, 506, 880
Beuermann, K., et al. 1995, A&A, 294, L1
Cowley, A. P., Schmidtke, P., Crampton, D., & Hutchings, J. B. 1998, ApJ, 504, 854
Crowther, P. A., & Bianchi, L. 2001, in preparation
Deufel, B., Barwig, H., Simic, D., Wolf, S., & Drory, N. 1999, A&A, 343, 455
Feldman, P. D., Sahnow, D. J., Kruk, J. W., Murphy, E. M., & Moos, H. W. 2001, J. Geophys. Res., 106, 8119
Gaensicke, B. T., Beuermann, K., & de Martino, D. 1996, in Lecture Notes in Physics 472, Supersoft X-Ray Sources, ed. J. Greiner (Berlin: Springer), 105
Gaensicke, B. T., van Teeseling, A., Beuermann, K., & Reinsch, K. 2000, NewA Rev., 44, 143
Greiner, J. 1996, in Lecture Notes in Physics 472, Supersoft X-Ray Sources, ed. J. Greiner (Berlin: Springer), 299
Greiner, J., & Wenzel, W. 1995, A&A, 294, L5
Matsumoto, K. 1996, PASJ, 48, 827
McGrath, T. K., Schmidtke, P. C., Cowley, A. P., Ponder, A. L., & Wagner, R. M. 2001, AJ, 122, 1578
Meyer-Hofmeister, E., Schandl, S., Deufel, B., Barwig, H., & Meyer, F. 1998, A&A, 331, 612
Moos, H. W., et al. 2000, ApJ, 538, L1
Sahnow, D. J., et al. 2000, ApJ, 538, L7
Tomov, T., Munari, U., Kolev, D., Tomasella, L., & Rejkuba, M. 1998, A&A, 333, L67
Will, T., & Barwig, H. 1996, in Lecture Notes in Physics 472, Supersoft X-Ray Sources, ed. J. Greiner (Berlin: Springer), 99